# Observations and Analysis of Fatigue Crack Growth in Circular Notched Polyethylene Specimens

**Byoung-Ho Choi[1,*], Ilhyun Kim[1], Yongjian Zhao[1], Ji Mi Lee[1] and Alexander Chudnovsky[2]**

[1] School of Mechanical Engineering, Korea University, Seoul, 136-701, Republic of Korea
[2] Department of Civil and Materials Engineering, University of Illinois at Chicago, Chicago, IL 60607, U.S.A.
* Corresponding author: bhchoi@korea.ac.kr

**Abstract** Many fundamental as well as technical issues with PENT (ASTM F2136) are identified, for instance the inability of separating crack growth from crack initiation, too long duration of the test for new generation of PE, outdated test conditions unchanged since the original formulation designed for old PE materials, etc. Therefore, there is a quest for a new accelerated test method. Recently, a circular notched specimen (CNS) has been proposed as an accelerated fatigue testing. However, formation of an asymmetric crack in CNS and early transition to a ductile failure limit the applicability of CNS test for studies of SCG. There are several factors responsible for the asymmetry of SCG. Especially, geometric misalignments of CNS are the most common practical weakness of the test. The present paper reports the observation of asymmetric SCG in CNS under fatigue conditions and analysis by finite element method (FEM) of the CNS misalignments effect on the crack growth asymmetry. Root causes of the asymmetric crack growth and its effect on the time to failure (fatigue lifetime) are discussed.

**Keywords** Fatigue, Polyethylene, Crack path, Crack growth, Circular notched specimen

## 1. Introduction

Plastic pipes have become popular in the pipe industry owing to their distinct advantages, which include low cost, low weight, good impact resistance, flexibility, and chemical resistance. However, it is known that plastic gas pipes such as polyethylene (PE) pipes do not have enough crack growth resistance to both ductile and brittle fracture as compared to metal gas pipes. To solve these critical problems, the plastic industry has dedicated a lot of effort to improving the crack growth resistance of pipe-grade PE to both ductile and brittle fracture. As a result, PE100/PE125-grade PE gas pipe resin has been developed by several PE resin manufacturers. However, current test standards for characterizing the crack growth resistance of PE are inadequate owing to the unique crack growth characteristics of PE. The American Society for Testing and Materials (ASTM) and the International Organization for Standardization (ISO) have proposed a few standard test methods for quantifying the resistance to slow crack growth of commercial pipe-grade polymeric materials such as PE [1].

However, since current test methods only suggest the recording of the time to failure, it is impossible to observe the response of the deformation and/or the crack growth behavior of the sample during tests. Consequently, most current test standards cannot distinguish between crack initiation and crack growth, which necessitates a new experimental method. The PENT test is suggested in ASTM as a standard test method for evaluating slow crack growth in PE materials [1], but this test lacks the capability to separate the crack propagation and crack initiation characteristics. Moreover, this test is designed only for a single stress level (2.4 MPa) based on old PE material and, therefore, there has been some criticism surrounding this standard. In stage II, it may be important to understand the crack initiation and crack propagation, and these should be addressed separately. In cases of crack propagation determining brittle fracture, there have been many experimental and analytical results, and the crack layer theory [2,3,4] is promising in predicting the complex continuous/discontinuous crack propagation observed in polyethylene. Meanwhile, studies of crack

initiation are relatively scarce due to uncertainty of its mechanism [5]. To solve these problems, some researchers have recently developed a new test that uses a circular notched specimen (CNS) (Fig. 1) to characterize the crack growth resistance and rank PE materials. Numerical investigation of the distribution of the stress intensity factors (SIFs) in CNS has been conducted in [6]. The advantage of the CNS is its moderate processing cost and the ease of fabricating the precrack. The front of the circular notch in the CNS is under triaxial stress conditions, making it possible to generate the highest effective stress, so accelerated tests can therefore be performed under any loading conditions. As a result, research of crack initiation and propagation using CNS is in progress [7,8,9]. However, it is also known that CNS create a problem for characterizing the crack growth behavior of brittle materials, because the crack growth is seldom axisymmetric [10]. In Fig. 2, experimentally observed cases of practically symmetric and typically asymmetric crack growth of PE in CNB specimens are shown [10]. Zhao et al. [10] reported that even initial imperfections in material or specimen geometry may strongly affect final time to failure, and asymmetrical fatigue crack propagation is easily changed in a severely distorted asymmetric manner. This can be critical as once asymmetric crack propagation takes place, recorded time to failure is shorter than that of symmetrical crack growth with all other parameters being the same. Moreover, as described above, the degree of asymmetry increases with crack propagation. As a result, the observed slope of S-N curve for time to failure may not represent the true fatigue behavior of the material, as it depends on specimen geometry imperfections. In other words, the crack growth process is highly sensitive to the variations of specimen geometry. In contrast with that, the crack initiation time is much less sensitive to geometry, except for notch depth variation Therefore it is more reasonable to use CNS testing for ranking materials with respect to the fatigue crack initiation resistance.

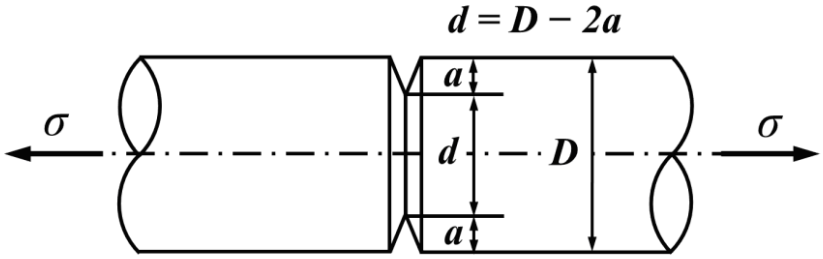


Fig. 1 Geometry of a circular notched specimen (CNS)

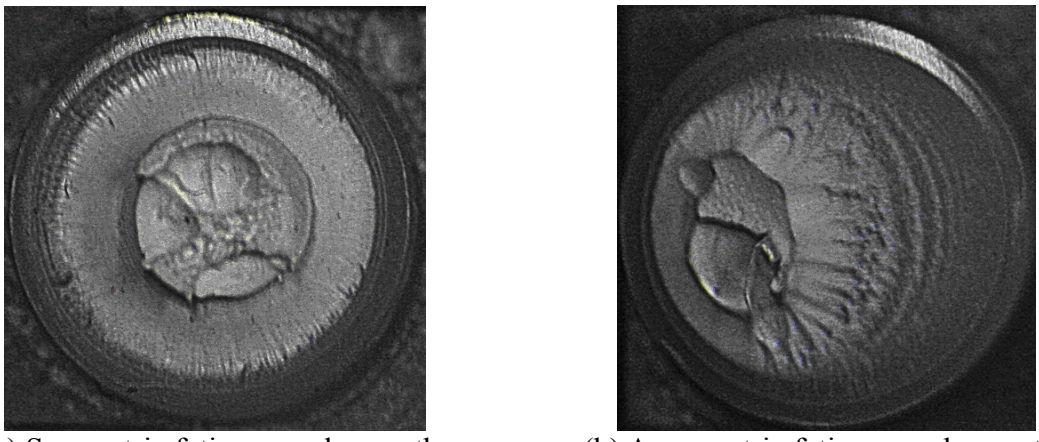

(a) Symmetric fatigue crack growth (b) Asymmetric fatigue crack growth

Fig. 2 Two typical types of fatigue crack growth in CNS

Many technical issues such as the notch sensitivity (brittleness), the anisotropy of the specimen, the initial notch geometry, and the geometric alignment of the centerline of the specimen and the notch should be considered in the interpretation of experimental data for asymmetric crack formation [11].

The effects of two types of noncircular initial notch geometries of a CNB specimen, i.e., the misalignment of the centerlines of the specimen and the notch, and the ellipticity of the notch—on the crack growth behavior have been previously studied by the authors [11]. In addition, the geometric misalignment of the CNB specimen in the experimental setup is also a critical issue. There are two types of geometric misalignment:concentric and angular misalignments as well as a combination of two.— The individual effects of concentric and angular misalignments on the crack growth behavior were considered. The effect of the geometric misalignments of PE on crack growth behavior at the early stage is not very significant, but an asymmetric crack gradually develops as the crack grows.

In this study, the effects of various geometric misalignments of CNB specimens on the fatigue crack growth behavior of pipe-grade PE were investigated by three-dimensional (3D) numerical analyses. Combined misalignments (concentric and angular misalignments) and the effect of the direction of the angular misalignments (0, π/2, π, and 3π/2) of a CNB specimen were considered within the limitations of the practical difficulties created by test conditions. The variation of the SIFs with the progress of a two-dimensional (2D) crack under fatigue loading conditions based on the conventional Paris' equation was studied using 3D finite element analysis (FEA). In addition, the experimental observations of the asymmetric fatigue crack growth were compared with the 3D FEA results. Moreover, the effect of the asymmetric crack growth resulting from combined initial geometric misalignment on the lifetime to failure of the CNB specimen is also discussed.

## 2. Finite Element Analysis

The combined misalignment of the CNB specimen was studied by 3D FEA. The geometric misalignment,concentric, angular and their combination—were considered. The normalized concentric misalignment (e/R) was varied as 0, 0.004, 0.012, and 0.020, using CNB specimens of radius (R) 5 mm. At the same time, the angular misalignment ($e_\theta$) was varied as 0, 0.1, 0.2, and 0.4. The directions of the angular misalignments were 0, π/2, π, and 3π/2. Combined misalignment is the combination of concentric and angular misalignments. The three types of misalignments—i.e., concentric, angular, and combined—are shown in Fig. 3(a). Fig. 3(b) shows the directions of the angular misalignments (0, π/2, π, and 3π/2). The misalignment conditions of this study are summarized in Table 1.

Table 1 Summary of misalignment conditions

| | e/R | $e_\theta$ |
|---|---|---|
| Concentric misalignment | 0.004, 0.012, 0.020 | 0 |
| Angular misalignment | 0 | 0.1, 0.2, 0.4 |
| Combined misalignment | 0.004, 0.012, 0.020 | 0.1, 0.2, 0.4 |

A commercial FEA program, ABAQUS, were used for the FEA of a 3D model of the CNB specimens in this study. All the crack tips were remeshed for each calculation of the SIFs by considering their singularities. The element was of type C3D20 (a 20-node quadratic brick), and there were 60,000 elements and 250,000 nodes for each specimen. The physical properties of the material of the FEA are listed in Table 2.

The SIFs were calculated from 16 node points of the circular (notch) crack contour—at 0, π/8, π/4, 3π/8, π/2, 5π/8, 3π/4, 7π/8, π , 9π/8, 10π/8, 11π /8, 3π/2, 13π/8, 7π/4, 15π/8, and 2π. Based on the

calculated SIF at each node, the amount of crack growth for each node was defined using the conventional Paris equation with constants C = 1 x $10^{-11.6}$ and m = 4 [4], as shown in Table 2, with the assumption of a fatigue interval of $10^5$ cycles.

The critical SIF ($K_c$) was 75.7 MPa·$mm^{1/2}$, which was obtained from the experimental results of fractured CNB spec-imens with symmetric crack growths [19]. The lifetime to failure (termination of the crack-growth simulation) was determined when the SIF of any node point of the circular (notch) crack contour reached the critical SIF. The direc-tion of the crack growth was determined as the normal to the tangent to the circular crack (notch) contour based on the maximum tangential stress (MTS) criterion [20], as shown in Fig. 4.

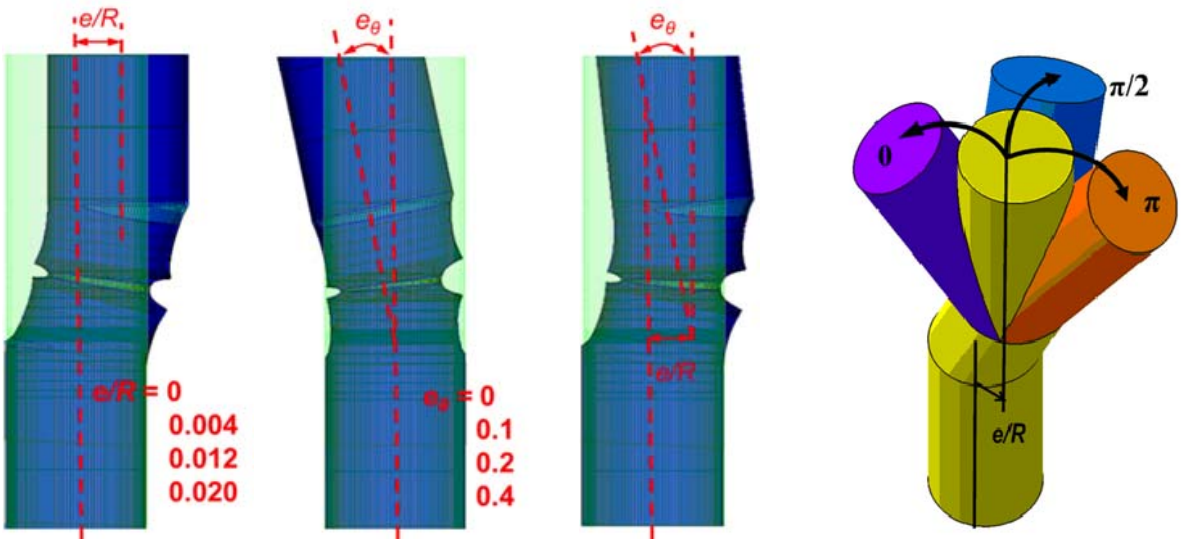


(a) Combined misalignments (Concentric+Angular) (b) Direction of angular misalignment

Fig. 3 Definition of combined misalignments

Table 2 Physical properties of the material

| Young's modulus, $E$ ($MPa$) | Poisson's ratio, $v$ | Constant for Paris' equation, $C$ | Constant for Paris' equation, $m$ | Remote stress range, $\Delta\sigma$ ($MPa$) |
|---|---|---|---|---|
| 1250 | 0.4 | $10^{-11.6}$ | 4 | 10.8 |

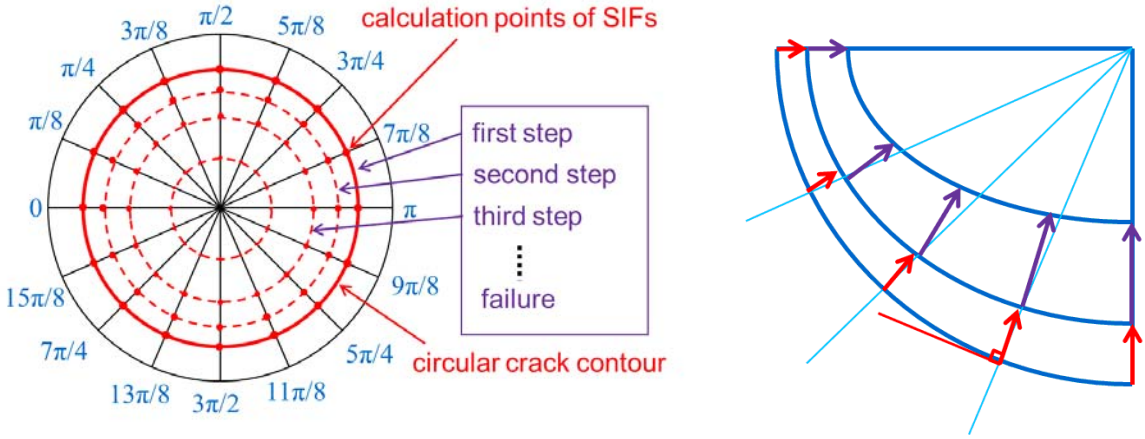


(a) Crack growth steps and crack tip locations (b) Modeling of crack growth

Fig. 4 Modeling of crack growth of CNS in FEA

## 3. Results and Discussions

The accuracy of the FEA was confirmed by comparing the SIFs calculated using FEA for a symmetric crack with those calculated using an analytical solution. The analytical expression of the SIFs of a CNB specimen was as expressed as below.

$$K = \frac{1}{2}\sigma_{net}\sqrt{\frac{\pi a d}{D}}\left(1+\frac{1}{2}\lambda+\frac{3}{8}\lambda^2-0.363\lambda^3+0.731\lambda^4\right)\cdot\left(1+0.1\sqrt{\frac{2a}{D}}\left(1-\frac{2a}{D}\right)\right), \quad (1)$$

where, $\sigma_{net}$ is the net section stress, and a and D are respectively the crack length and diameter (d = D - 2a, λ = d/D). It was observed that the SIFs obtained from the FEA and the analytical solution were almost identical.

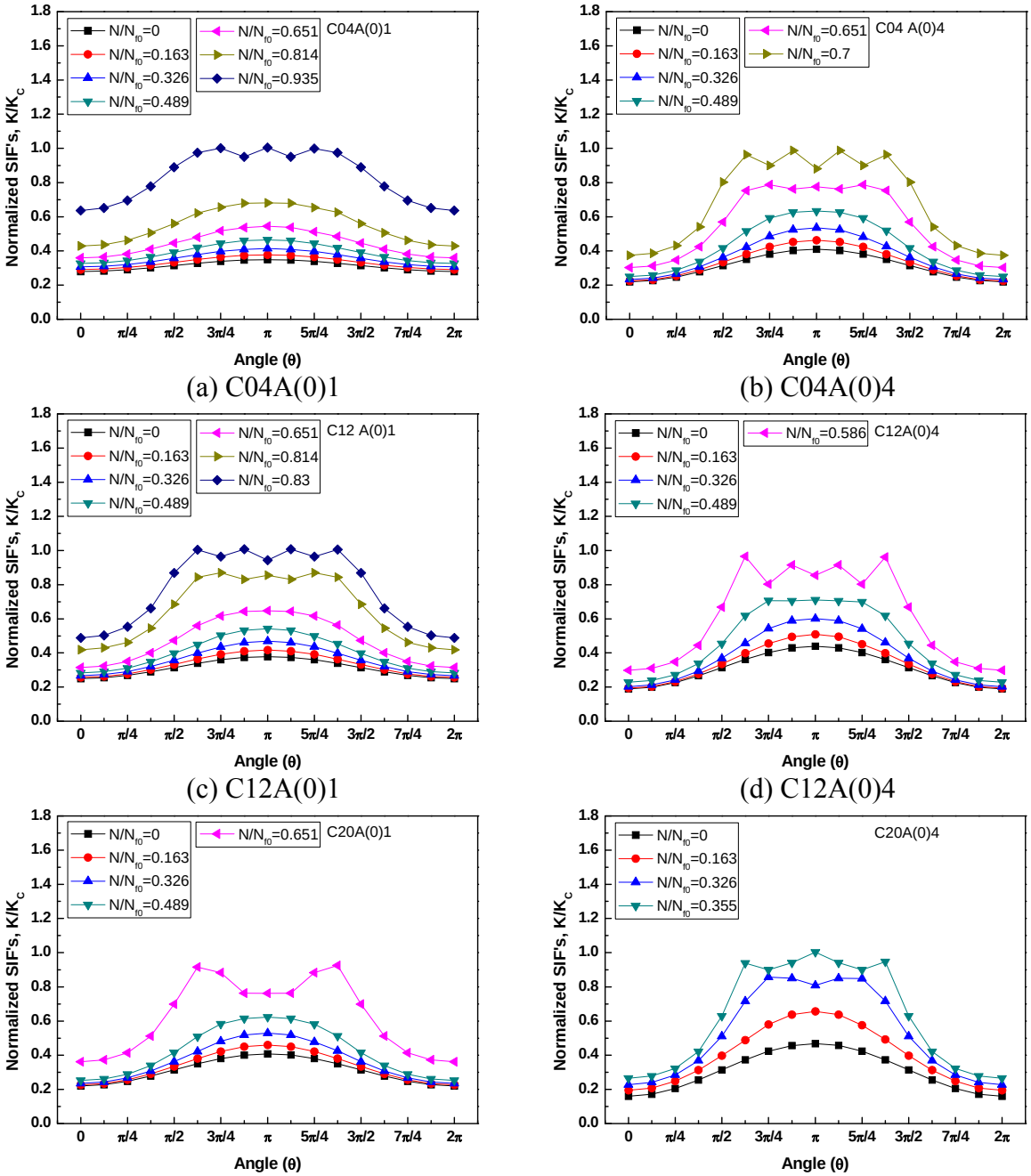


(a) C04A(0)1 (b) C04A(0)4

(c) C12A(0)1 (d) C12A(0)4

(e) C20A(0)1 (f) C20A(0)4

Fig. 5 The variation of normalized SIFs at the circular crack contour for '0' angular direction

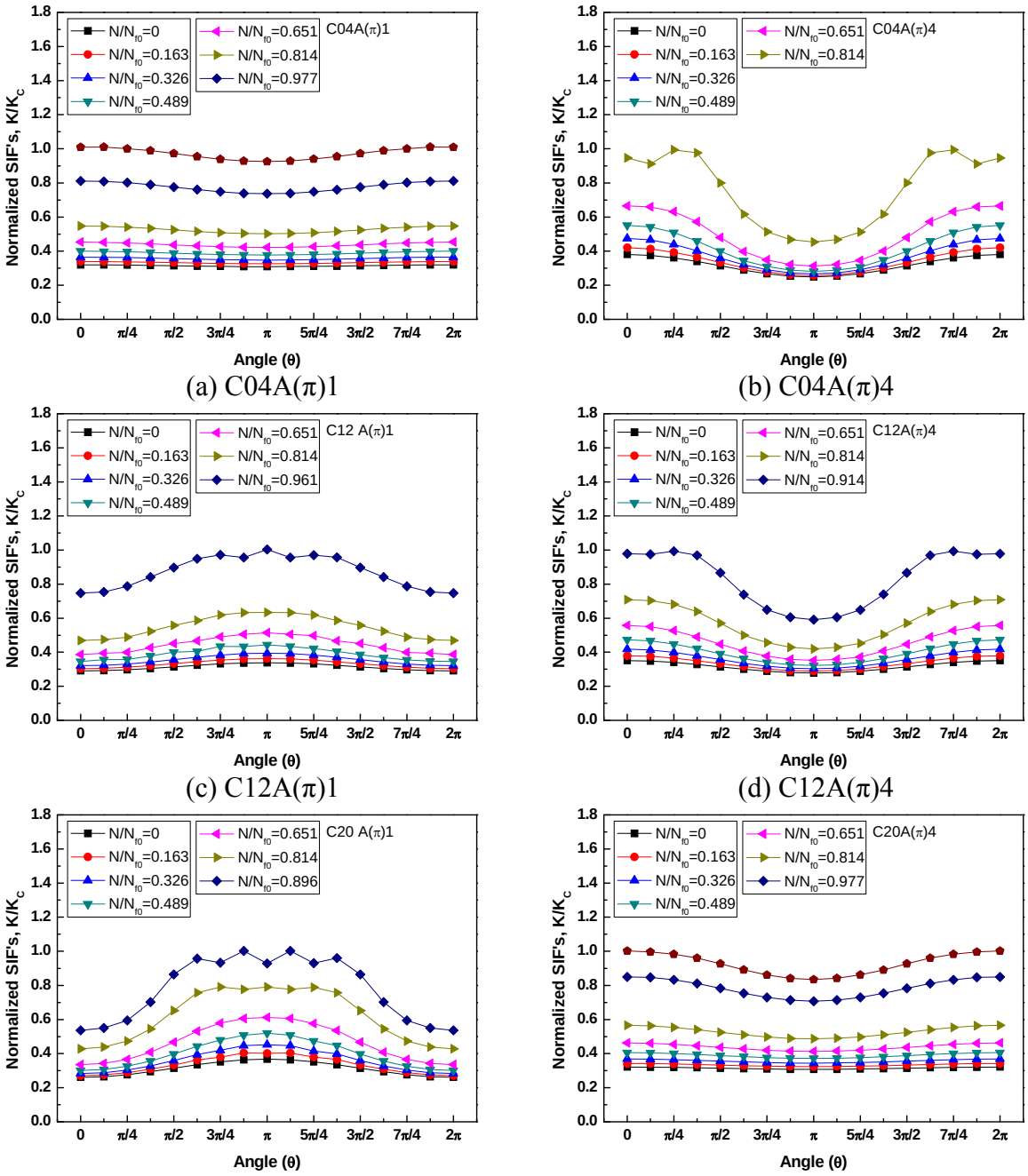


(a) C04A(π)1 (b) C04A(π)4

(c) C12A(π)1 (d) C12A(π)4

(e) C20A(π)1 (e) C20A(π)4

Fig. 6 The variation of normalized SIFs at the circular crack contour for 'π' angular direction

Combined misalignment (concentric and angular misalignments) and the effect of the directions of the angular mis-alignments (0, π/2, π, and 3π/2) of the CNS specimens were considered within the limitations of the practical difficulties of test conditions.

Fig. 5 shows the FEA results of the variation of the SIFs around the crack contour with a concentric misalignment (e/R) of 0.004-0.020 and angular misalignment ($e_\theta$) of 0.1 and 0.4. For all cases, the direction of the angular misalignment was 0. There were only little differences in the initial SIFs, but the difference between the maximum and minimum SIF values rose as the crack grew. As expected, the maximum SIF was observed at $\theta = \pi$ and the minimum was observed at $\theta = 0$. It was also observed that when the directions of the concentric and angular misalignments were opposite, their effects neutralized each other and the normalized time to failure at high speeds decreased as

the angular misalignment increased. This means that when the direction of the angular misalignment was 0, the directions of the concentric and angular misalignments were actually opposite to each other. However, when the concentric misalignment was small, the two cases of angular misalignments of 0.1 and 0.4 early during the crack propagation had small differences between the maximum and minimum SIF values. However, as the misalignment became noticeable, the difference increased and exceeded those of other cases of the crack propagation. It could be concluded that these large differences at the early stage accelerated the crack propagation and decreased the lifetime.

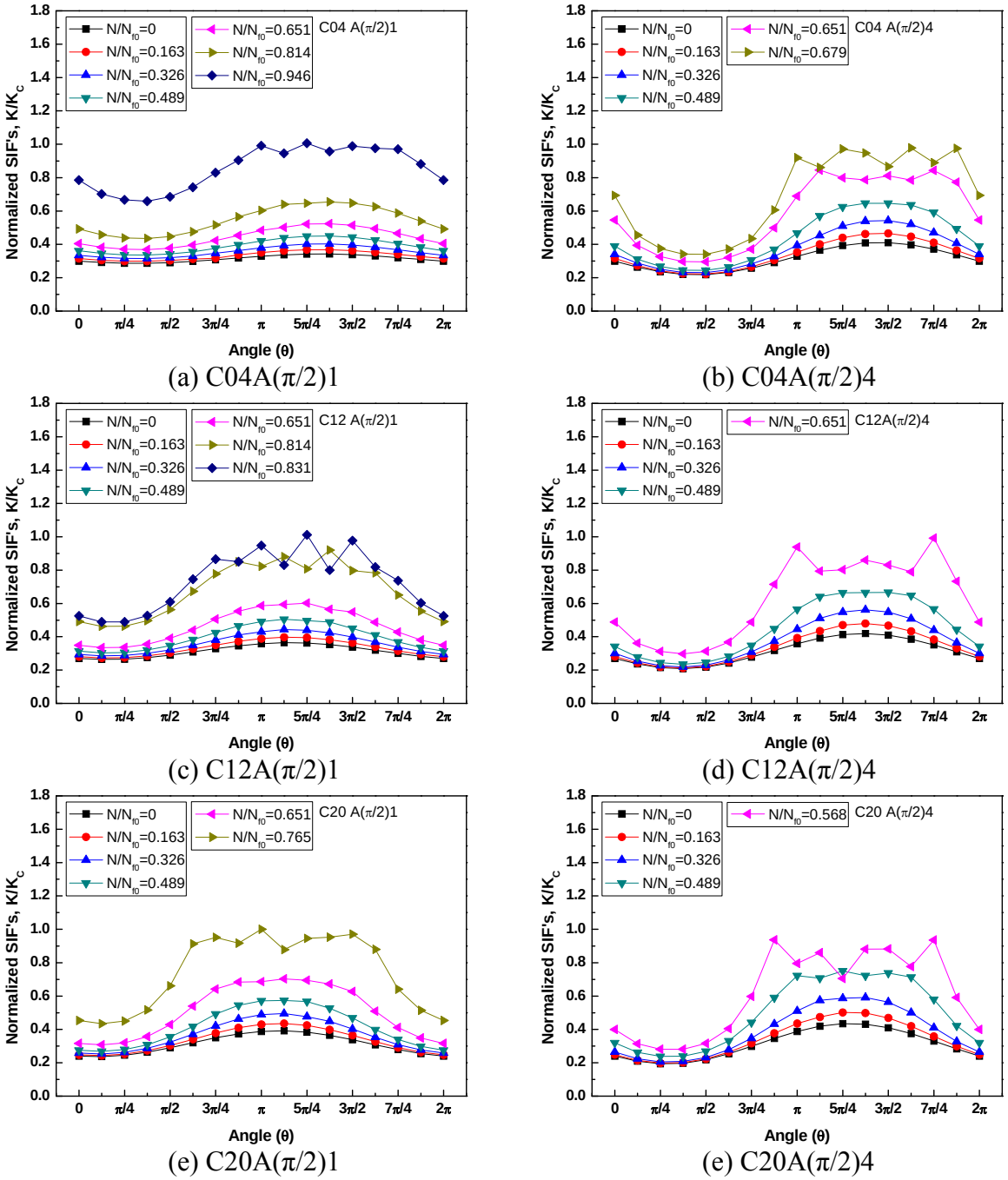


(a) C04A(π/2)1 (b) C04A(π/2)4

(c) C12A(π/2)1 (d) C12A(π/2)4

(e) C20A(π/2)1 (e) C20A(π/2)4

Fig. 7 The variation of normalized SIFs at the circular crack contour for 'π/2' angular direction

Fig. 6 shows the FEA results of the variation of the SIFs around the crack contour for various concentric misalignments (e/R) ranging from 0.004 to 0.200, angular misalignments ($e_\theta$) ranging from 0.1 and 0.4, and angular misalignment direction of π. The angular misalignment direction of π

means that the concentric and angular misalignments were in the same direction. As the concentric misalignment increased, the stress distribution of the angular misalignment showed a different tendency. Although the angular misalignment was 0.1, the difference between the maximum and minimum SIF values was still small. Nevertheless, the asymmetric crack growth developed gradually as the concentric misalignment increased (see Figs. 6(a), 6(c), and 6(e)). It was also observed that as the concentric misalignment increased, the top positions of the maximum and minimum SIFs became upside down. However, when the angular misalignment was 0.4, the difference between the maximum and minimum SIF values was large at the early stage, and then gradually decreased as the concentric misalignment increased (see Figs. 6(b), 6(d), and 6(f)). Moreover, although the concentric misalignment increased, the top positions of the maximum and minimum values were not upside down; only their difference decreased. Based on these results, it can be understood that if the angular misalignment increased beyond 0.4, $K/K_c$ became 1, after which the positions of the maximum and minimum SIF values were reversed and their difference further increased. From this result, it can be deduced that eθ rather than e/R influences the crack growth rate.

Fig. 7 shows the FEA results of the variation of the SIFs around the crack contour for various concentric misalignments (e/R) ranging from 0.004 to 0.020 and angular misalignments ($e_\theta$) ranging from 0.1 and 0.4 when the direction of the angular misalignment was π/2. The angular misalignment direction of π/2 means that the concentric and angular misalignments were perpendicular to each other. It could be observed that the distribution of the SIFs around the crack contour shifted from the previous combination of misalignments. When the angular misalignment was 0.1, the SIFs around the crack contour did not change significantly (see Figs. 7(a), 7(c), and 7(e)). However, the distribution of the SIF around the crack contour varied more significantly. It could thus be deduced that the lifetime to failure varied somewhat as the direction of the angular misalignment changed. The distribution of the SIFs and the lifetime to failure were determined by the two misalignments. In other words, the direction of the misalignments could be critical to the reliability of the test results when using CNB specimens.

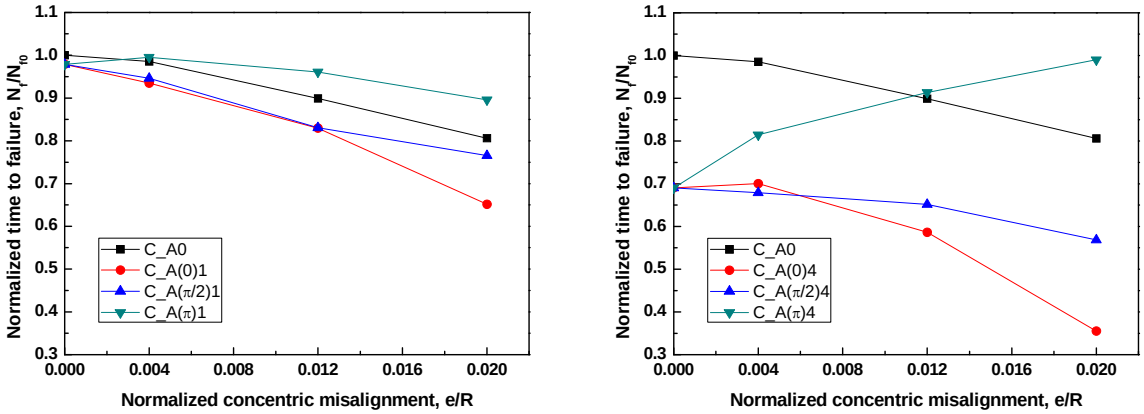


(a) $e_\theta$=0.1 (b) $e_\theta$=0.4

Fig. 8 Variation of the normalized time to failure under combined misalignments

Fig. 8 shows the variation of the normalized time to failure under combined misalignments. When the direction of the angular misalignment was 0, the lifetime to failure decreased regardless of the misalignment conditions. However, when the direction of the angular misalignment was π, the lifetime to failure increased up to a certain level for concentric misalignment. These results were because the concentric and angular misalignments simultaneously determined the distribution of the SIFs of the crack contour. The contributions of the two misalignments can therefore be varied. For example, when the direction of the angular misalignment was π, the shape of the asymmetric crack

growth for the concentric misalignment was opposite to that for the angular misalignment. Several other factors, such as the notch sensitivity (brittleness), anisotropy of the specimen, and notch geometry can also affect the lifetime to failure and the asymmetric crack growth of CNB specimens. However, it is clear that geo-metric misalignments of CNB specimens can significantly affect the crack growth behavior and the lifetime to failure. Therefore, it can be noticed that the installer should be careful to avoid any unintentional misalignment of the CNB specimen in order to produce reliable test results.

## 3. Conclusions

In this study we investigated the effects of various geometric misalignments of CNB specimens on the fatigue crack growth behavior of pipe-grade PE by means of three-dimensional (3D) numerical analyses. Combined misalignments (concentric and angular misalignments) and the effect of the direction of the angular misalignments (0, $\pi/2$, $\pi$, and $3\pi/2$) of a CNB specimen were considered within the limitations of the practical difficulties created by test conditions.

The distribution of the SIF changed with a change in the direction of the misalignments, so the lifetime to failure under combined misalignments could be varied depending on the status of the combined misalignment. For example, the time to failure increases as the angular misalignment in the direction of $\pi$ increases, for up to 2% concentric misalignment of the radius of the CNB specimen It is not clear. On the contrary, the normalized time to failure for a combination of 2% concentric misalignment and 0.4 angular misalignment decreased by almost 65% compared to that without any misalignment.

Several other factors, such as notch sensitivity (brittleness), anisotropy of the specimen, and notch geometry can also affect the lifetime to failure and asymmetric crack growth in CNB specimens. However, it is clear that geometric misalignments of the specimens significantly affect the crack growth behavior and the lifetime to failure. Such sensitivity of the test results to various misalignments limit the potential of considering this test as a standard.

**References**

[1] X. Lu, R. Qian, N. Brown, Discontinuous crack growth in polyethylene under a constant load. J Mater Sci, 26 (1991) 917–924.
[2] A. Chudnovsky, Crack layer theory, NASA Report #174634, 1984.
[3] A. Chudnovsky, Y. Shulkin, Application of crack layer theory to modeling of slow crack growth in polyethylene. Int J Fract 97 (1999) 83-102.
[4] B.-H. Choi, W. Balika, A. Chudnovsky, G. Pinter, R.W. Lang, The use of crack layer theory to predict the lifetime of the fatigue crack growth of high density polyethylene, Polym Eng Sci 49 (2009) 1421-1428.
[5] A. Chudnovsky, B. Kunin, A probabilistic model of brittle crack formation. J Appl Phys 62 (1987) 4124-4129.
[6] Y. Lei, B.K. Neale, Non-linear, axi-symmetric finite element analyses of a circumferentially cracked bar specimen. Int J Pressure Vessels Piping 73 (1997) 199–210.
[7] V. Favier, T. Giroud, E. Strijko, J.M. Hiver, C. G'Sell, S. Hellinckx, A. Goldberg, Slow crack propagation in polyethylene under fatigue at controlled stress intensity. Polymer 43 (2002) 1375–1382.
[8] A. Frank, W. Freimann, G. Pinter, R.W. Lang, A fracture mechanics concept for the accelerated characterization of creep crack growth in PE-HD pipe grades. Eng Fract Mech 76 (2009) 2780–2787.
[9] W. Zhou, B.-H. Choi, A. Chudnovsky, Crack initiation in pipe grade polyethylene, in:

Proceddings of SPE/ANTEC 2006. Charlotte, NC, USA: Society of Plastics Engineers, 2006, pp. 2485-2489.

[10] B.-H. Choi, Y. Zhao, Evaluation of the crack initiation characteristics of pipe grade polyethylene under fatigue loads, in: Proceedings of ANTEC 2010. Orlando, FL, USA: Society of Plastics Engineers, 2010. pp. 1644–1648.

[11] Y. Zhao, I. Kim, B.-H. Choi, J.-M. Lee, Variation of the fatigue lifetime with the initial notch geometry of circular notched bar specimens. Int J Fract 167 (2011) 127–134.